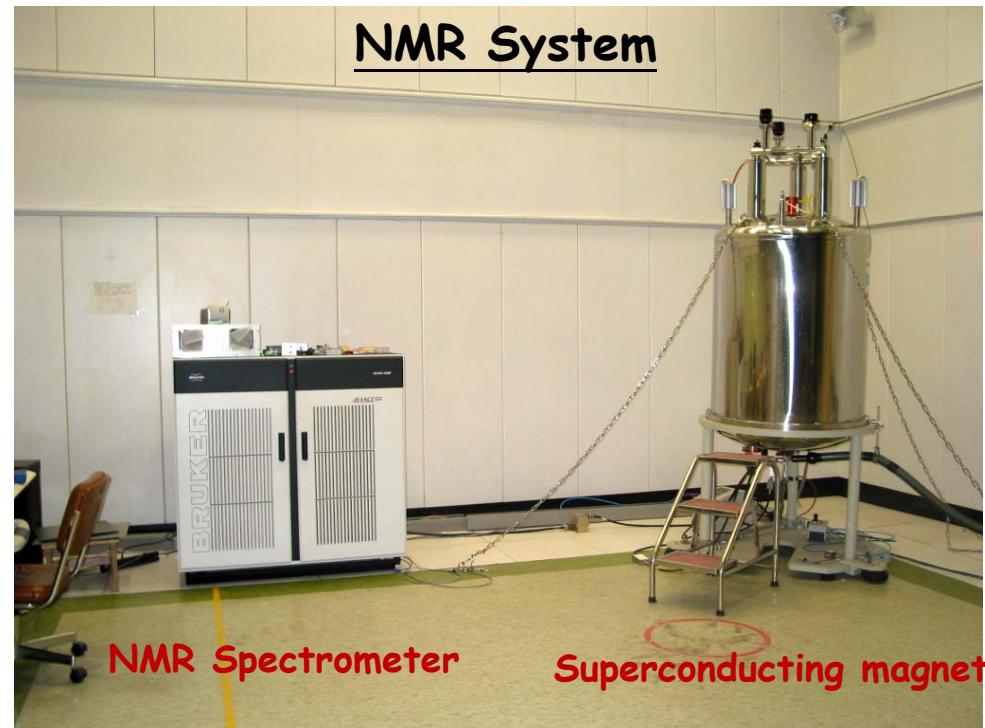
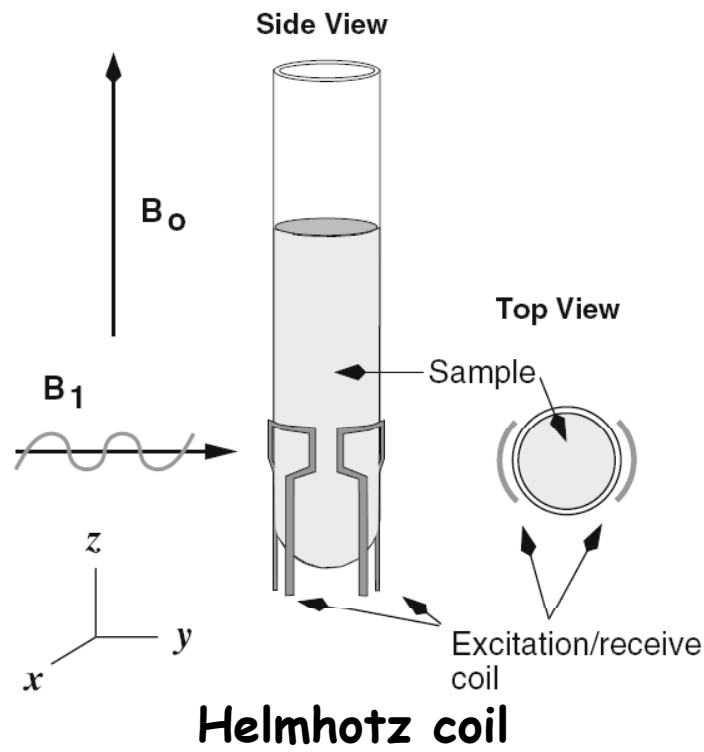


1.3 Detection of Nuclear Spin Transitions

- The presence of static field caused the spins to occupy different energy states
- To detect the magnetization one need to apply a RF field of frequency equal to the Larmor frequency in the orthogonal direction to the static field.



2.2.9 Setting the Receiver Gain

Too high or too low will produce signal distortion. (Place strongest signal to full scale)

Resolution of an analog-to-digital converter (ADC): xx bit ADC.

N bit ADC means divide the full signal into 2^N divisions. Example: 4 bit ADC will have resolution of $5V/2^4 = 0.3125$ Volts /division for a full signal of 5 Volts. Any signal lower than 0.3125 V will be treated as 0 and cannot be detected. But if the signal is detected with a 10 bit ADC the resolution will be $5/2^{10} \sim 0.005$ V. The higher the ADC resolution the better we can detect weak signal.

Water concentration: 110 M and sample concentration: 1 mM (About 10^{-5} of water signal)

ADC bits needed: 17 bit → Water (solvent) signal suppression is needed.

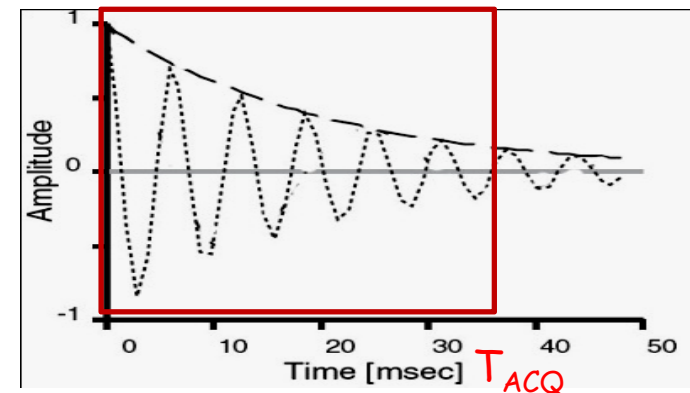
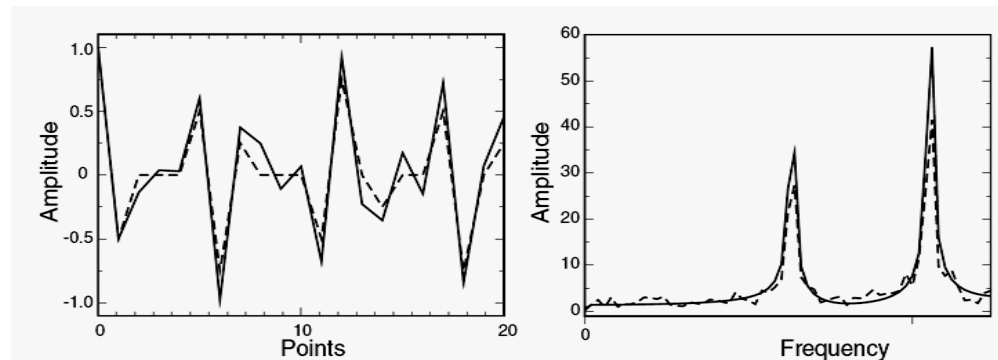
2.2.10 Spectral Resolution and Acquisition Time of FID

Spectral resolution depends on the total acquisition time (T_{ACQ}):

$$T_{ACQ} = \text{number of points} \times DW$$

The true, or actual, resolution of the spectrum is defined by the *observed Linewidths* of the resonances, which depends on both the intrinsic linewidths of the resonances and the spectral resolution defined by T_{ACQ} . Consequently, any peaks that are closer than $\approx 1/(\pi T_2) + 2/T_{ACQ}$. Cannot be resolved because their observed linewidths exceed their frequency separation.

Digital resolution: SW/N



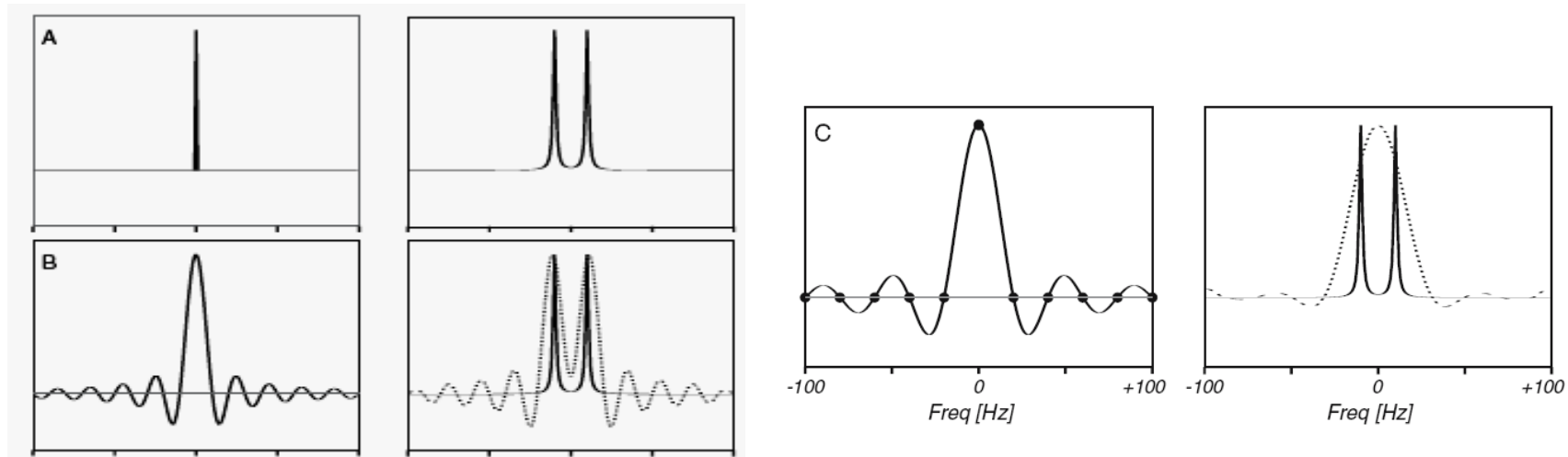


Figure 2.18. Acquisition time and spectral resolution. The effect of the acquisition time on the corresponding to increasingly shorter acquisition times. The peak separation is 20 Hz and the intrinsic linewidths of each peak is 2 Hz. Rows A, B, and C represent acquisition times of 2 sec, 100 msec, and 50 msec, respectively. The left panels show the Fourier transform of the square waves that corresponds to each acquisition time. The right panels show the true spectra as solid lines and the convolution of the spectra with the sinc function as dotted lines. When the acquisition time is 2 sec (A), there is essentially no additional broadening of the resonances by the convolution with the sinc function. When an acquisition time of 100 msec is used (B), the lines are broadened by approximately 20 Hz, but they are still resolved. When the signal is acquired for only 50 msec, the additional broadening is approximately 40 Hz and the individual lines are no longer resolved. The 'wiggle' patterns that are introduced to the spectra by the transform of the square wave may not be observed in the final spectrum because the sampling frequency of the spectrum (SW/n) is such that only the zero-crossing points of the sinc function are sampled (see Panel C). Increasing the digital resolution, by adding more points, will cause these wiggles to appear in the spectrum.

2.2.10.1 Scan Repetition Rate:

Due to The steady state signal for a repetition rate ρ $A \approx A_0(1 - e^{-T/T_1})$

The Optimal pulse angle depends on the ratio of the scan repetition rate to spin-lattice relaxation time according to the following equation, derived by Ernst et al [53]:

$$\cos \beta_{opt} = e^{-T/T_1}$$

Dummy scan: The scans for establishing steady state before data acquisition.

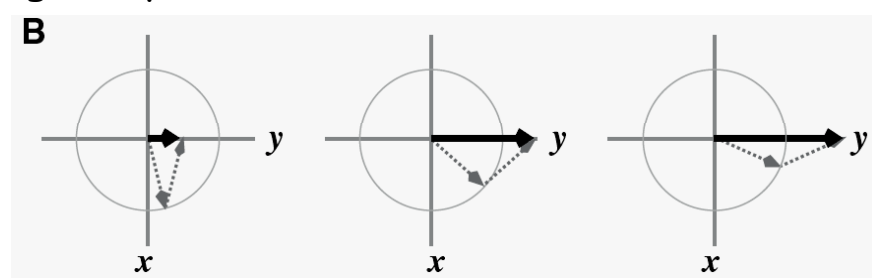
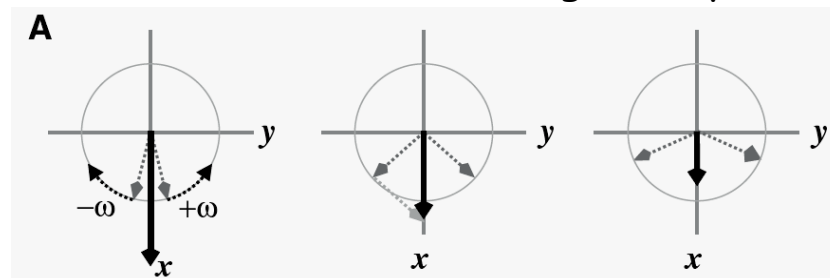
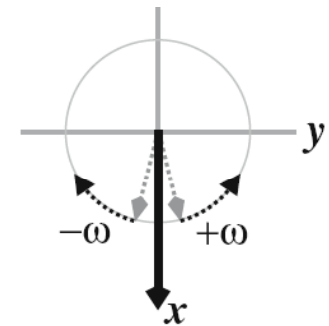
2.3 Experimental 1D-pulse Sequence: Pulse and Receiver phase

2.3.1. Phase Cycle: The process of acquiring data with different pulse and receiver phases is called phase cycling. The phase of the excitation pulse and the phase of the receiver are changed in a defined way over a number of scans. Phase cycling is essential in suppressing artifacts and in selecting coherences.

2.3.1.1 Phase of the RF-pulse: $P_x = \cos(\omega t) = \frac{1}{2} [e^{i\omega t} + e^{-i\omega t}]$

$$P_{x+\pi/2} = \frac{1}{2} [e^{i(\omega t+\pi/2)} + e^{-i(\omega t+\pi/2)}] = \frac{1}{2} [i e^{i\omega t} - i e^{-i\omega t}] = \sin(\omega t)$$

Cos(ωt) can be represented as two circularly polarized waves rotating at opposite directions. Sum of them give a pulse along the X-axis and subtraction gives a pulse along the y-axis

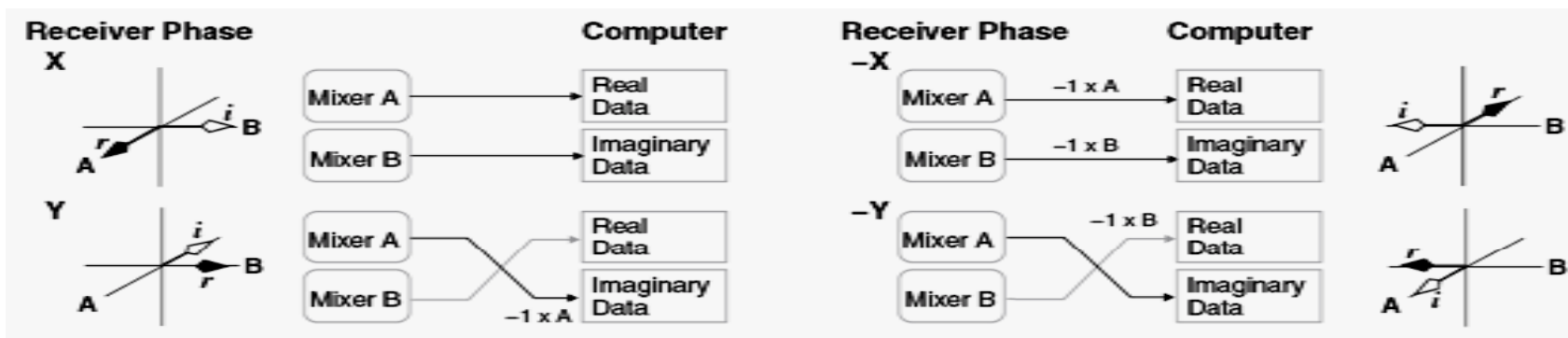


Although it is convenient to associate the direction of the pulse with a particular axis in space, there is no absolute coordinate system for the direction of the x- and y-pulses and it is not possible to specify in absolute terms that a particular direction in space is the x-axis. Rather, it is the relative phase relationship between the pulses that defines their relative directions in space. For example, if an RF-pulse of $\cos(\omega t)$ is applied to the sample, followed by an RF-pulse of $\cos(\omega t + \pi/2)$, then the orientation of the B1 field of the second pulse will be shifted by 90° , relative to the B1 field of the first pulse.

Table 2.1. Effect of the pulse phase on the initial magnetization. The first column indicates the phase of the 90° pulse, the second column the resultant effect of this pulse on the magnetization, M_0 initially aligned along the z-axis. For example, a pulse along the y-axis tips the magnetization from the z-axis to the x-axis. This convention follows the 'right-hand rule', the direction of the pulse is along the thumb and the spins are tipped in the same direction as the curl of ones fingers. The last two columns indicate the resultant signals that would be observed along the x-axis and the y-axis while the magnetization precesses about B_0 . This assumes a counterclockwise precession of the bulk magnetization. Whether these signals would be interpreted as the real or imaginary component of the signal would depend on the receiver phase.

<i>Phase of Pulse</i>	<i>Effect of Pulse ($\pi/2$)</i>	M_x	M_y
0 [= x]	$z \rightarrow -y$	$M_0 \sin \omega t$	$-M_0 \cos \omega t$
1 [= y]	$z \rightarrow x$	$M_0 \cos \omega t$	$M_0 \sin \omega t$
2 [= -x]	$z \rightarrow y$	$-M_0 \sin \omega t$	$M_0 \cos \omega t$
3 [= -y]	$z \rightarrow -x$	$-M_0 \cos \omega t$	$-M_0 \sin \omega t$

Figure 2.21. Implementation of receiver phase. The signal routing paths for receiver phase values of x , y , $-x$, and $-y$ are shown in the center section of the diagram. The outer sections of the diagram indicate the magnetization measured by the two quadrature mixers, A and B. Mixer A is arbitrarily defined to always measure M_x and mixer B always measures M_y . These signals are routed to the computer memory differently, depending on the setting of the receiver phase. For each phase setting of the receiver the closed arrowhead indicates the direction of the real axis (r) while the open arrowhead shows the direction of the imaginary axis.



Receiver Implementation Phase

0 [= x]	The signal from mixer A is considered to be the real signal and the signal from mixer B is considered to be the imaginary signal.
1 [= y]	The signal from mixer A is multiplied by minus one and considered to be the imaginary signal while the signal from mixer B becomes the real signal (i.e. the output from the two mixers are switched and one is multiplied by minus one.)
2 [= -x]	The same signal pathway is used as above for a phase of x , except that both the real and imaginary signals are multiplied by minus one
3 [= -y]	Same as with a phase of y , except that the signal from mixer B is multiplied by minus one.

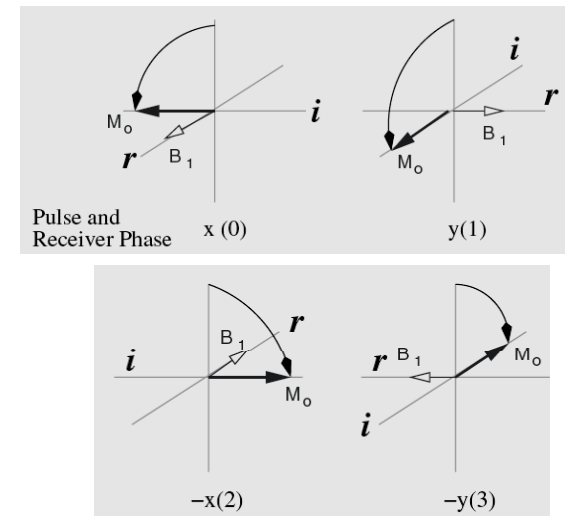
2.3.1.2 Receiver Phase

The receiver phase defines the relationship between the real and imaginary data channels of the digitized FID and a particular coordinate axis in the rotation frame. As with the phase of RF-pulses, the direction defined by a receiver phase of zero is arbitrary. It is the change in the receiver phase from scan to scan that is of importance. For illustrative purposes a receiver phase of zero will imply that the real component of the magnetization will represent the magnetization along the x-axis (M_x) and the imaginary component will represent the magnetization along the y-axis (M_y). If the phase of the receiver is shifted by 90° , the magnetization along the y-axis will be sent to the real data channel and magnetization along the negative x-axis will be sent to the imaginary data channel.

Changes in the receiver phase can be implemented in two ways, by direct alteration of the phase of the received signal by varying the phase of W_{IF} that enters the two mixers in the receiver, or by changing the routing of the signal from the two mixers to the computer. The 1st method is used for receiver phase shifts that are not multiples of 90° . The 2nd method is generally used to produce phase shifts in the receiver that are a simple multiple of 90° .

2.3.2 Phase Cycle and Artifact Suppression - Removal of artifacts due to both a DC offset in the FID as well as an imbalance of the quadrature detection channels.

Figure 2.22. Four-step phase cycle. The r and i indicate the real and imaginary data channels of the computer, respectively. The open-headed arrow represents the applied B_1 field. Note that the pulse is defined to be along the x-axis for the first scan, the y-axis for the next, and so on. The solid-head arrow indicates the bulk magnetization immediately after the pulse. The curved arrow indicates the trajectory of the magnetization during the pulse. After the pulse, the magnetization precesses counter-clockwise in the x-y plane.



2.3.2.1 Suppression of DC Offsets - Just apply a repetitive x, -x pulses is sufficient.

Data	Real Data	Imaginary Data	Data	Real Data	Imaginary Data
Scan 1 (Pulse & Rec. phase= x)	$-M_o \sin\omega t + DC$	$M_o \cos\omega t + DC$	Scan 1 (Pulse & Rec. phase = x)	$-M_o \sin\omega t$	$(1 + \eta)M_o \cos\omega t$
Scan 2 (Pulse & Rec. phase= -x)	$-M_o \sin\omega t - DC$	$M_o \cos\omega t - DC$	Scan 2 (Pulse & Rec. phase = y)	$-(1 + \eta)M_o \sin\omega t$	$M_o \cos\omega t$
Sum	$-2M_o \sin\omega t$	$2M_o \cos\omega t$	Sum	$-(2 + \eta)M_o \sin\omega t$	$(2 + \eta)M_o \cos\omega t$

2.3.2.2 Suppression of Imbalance in quadrature detection (need to cycle thru x and y)

- Imbalanced gains in the two channels: R channel $G = 1 + \eta$, I channel: $G = 1$

Then the signal will be: $(1 + \eta)\cos\omega t + i\sin\omega t = \eta\cos\omega t + e^{i\omega t}$

If we cycle the transmitter thru X- and Y-channels then after two pulses we have:

$$S(t) = (2 + \eta)M_o[-\sin\omega t + i\cos\omega t]$$

2.3.2.3 Cyclops: Suppression of DC offsets and Quad Imbalance:

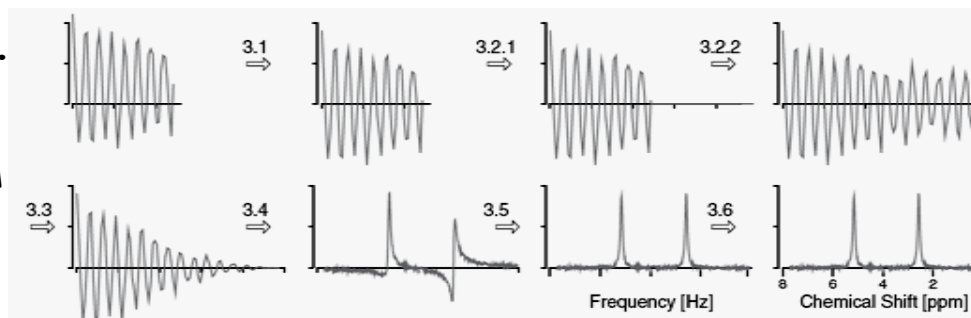
Shifting the pulse and receiver phases by π will remove DC offsets from the overall FID and a phase shift of $\pi/2$ will remove the effects of Quadrature imbalance. These two phase shifts can be combined into a complete phase cycle involving the following four steps of receiver phase and pulse phases: $0(=x)$, $-x$, $\pi/2(=y)$, $\pi(=-x)$, $3\pi/2(=-y)$. Note that this set of phases combines the two phase cycles such that for each phase of one artifact suppression phase cycle, all of the phases of the other artifact suppression cycle are applied. That is, a phase shift of 0 and $\pi/2$ for suppression of quadrature imbalance has been applied to each of the phase shifts that were used to remove DC offsets. The name of this simple phase cycle is **cyclops**, because the 'single eye' of the receiver follows the change in the direction of the magnetization that results from an equivalent phase shift of the pulse.

2.4 Exercises:

Chapter 3 INTRODUCTION TO SIGNAL PROCESSING

Figure 3.1. Overview of data processing.

1. Remove the DC offset.
2. Increase the resolution of the spectrum by zero-filling. N additional points are added to the end of the acquired data, giving $2N$ points.
3. Linear prediction (LP) replaces the zero-filled points with extrapolated data.
4. Apply an apodization function to remove the discontinuity from the end of the FID.
5. Fourier Transformation. The solvent line is removed by Linear prediction and errors in the initial data points are corrected prior to transformation.
6. Phase correct the spectrum to generate pure absorption peaks.
7. Reference the spectra using a chemical shift standard.

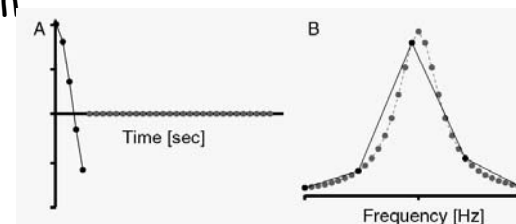


3.1: Removal of DC offset:

By phase cycling or by taking the average value of the last 10-20% points of the FID.

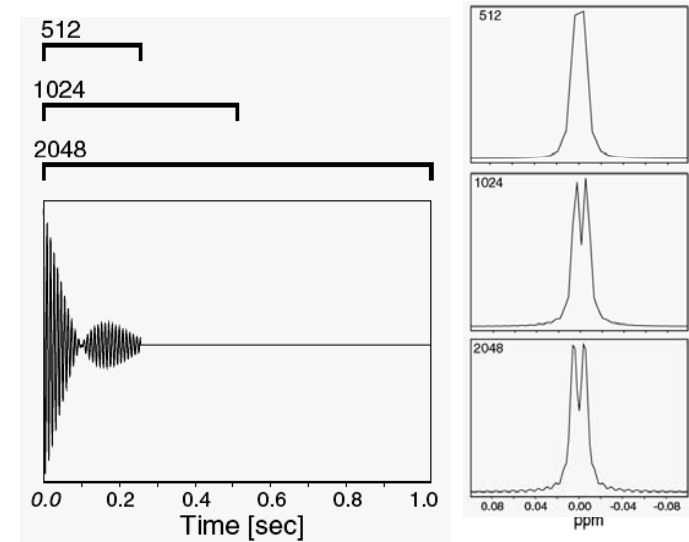
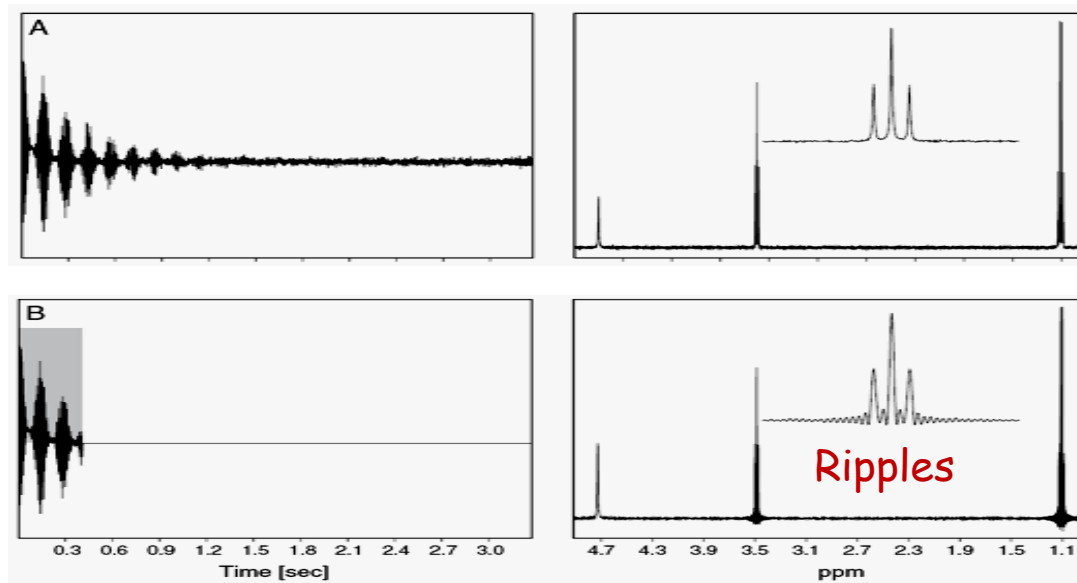
3.2. Increasing resolution by extending the FID: Data is often truncated before it decays to zero, especially in multi-dimensional expts. Truncation will degrade the resolution of the spectrum, introduce spectral artifacts, and can also result in a poor representation of the spectral lineshape due to the small number of points in the final spectrum.

Figure 3.2. Digital sampling. Panel A shows a FID consisting of five data points (black dots). Panel B shows the resultant spectrum from the Fourier transform of the five data point FID (solid black line). The gray dots in A are additional zero-filled points that have been added to the end of the FID. B shows the resultant spectrum (dotted line) after transforming the zero-filled FID.



3.2.1 Increasing Resolution by Zero-filling

3.2.1.1 Truncation artifact due to zero-filling



Increasing resolution by linear prediction: (Barhuijsen *et al.* [7].)

For an FID that can be represented by a sum of damped cosine functions:

$$x_n = \sum_{k=1}^K c_k e^{-n\Delta t/T_{2k}} \cos(\omega_k n\Delta t + \phi_k)$$

The n th point can be predicted from a linear combination of existing $n-1$ data points as:

$$x_n = a_1 x_{n-1} + a_2 x_{n-2} + \dots + a_M x_{n-M}$$

The most sensible use of linear prediction is to extend the FID by 20-40% and then use an apodization function to reduce the influence of the predicted points on the final spectrum.

3.3 Removal of truncation artifact: Apodization (Applying a window function)

The FID is brought to zero by multiplying the FID by an apodization function to give a modified FID. This process is termed apodization or applying a window function such as exponential, Lorentzian, Gaussian or trigonometric function.

3.3.1 Effect of Apodization on Resolution and Noise

In addition to removing truncation artifacts, the apodization functions will also affect the resolution and the signal-to-noise ratio of the spectra. For example, exponential multiplication leads to line broadening and a reduction in noise, while certain trigonometric functions produce narrowing of the spectral line with an increase in the noise. In general, these two effects are correlated. Efforts to increase the resolution of the spectra will also increase the noise. Apodization functions, such as exponential multiplication, that suppress signals late in the FID, will decrease the contribution of the noise to the Fourier transform. Unfortunately, they will also decrease the resolution of the spectrum. Conversely, functions that amplify signals late in the FID will increase the final resolution at a cost of increasing the noise.

3.3.1.1 Exponential multiplication:

The most common modification of the FID is exponential multiplication (EM), otherwise known as line broadening (LB). The EM apodization function simply multiplies the original FID by $e^{-t/a}$ to give the following apodized FID:

$$g(t) = e^{-t/T_2} e^{-t/a} = e^{-t[\frac{1}{T_2} + \frac{1}{a}]}$$

Fourier transformation of this function will produce a Lorentzian line, but with a modified T_2 that is shorter than the original T_2 :

$$\frac{1}{T_2'} = \frac{1}{T_2} + \frac{1}{a}$$

Or a line broadening of $\Delta\nu_{1/2} = 1/\pi a$

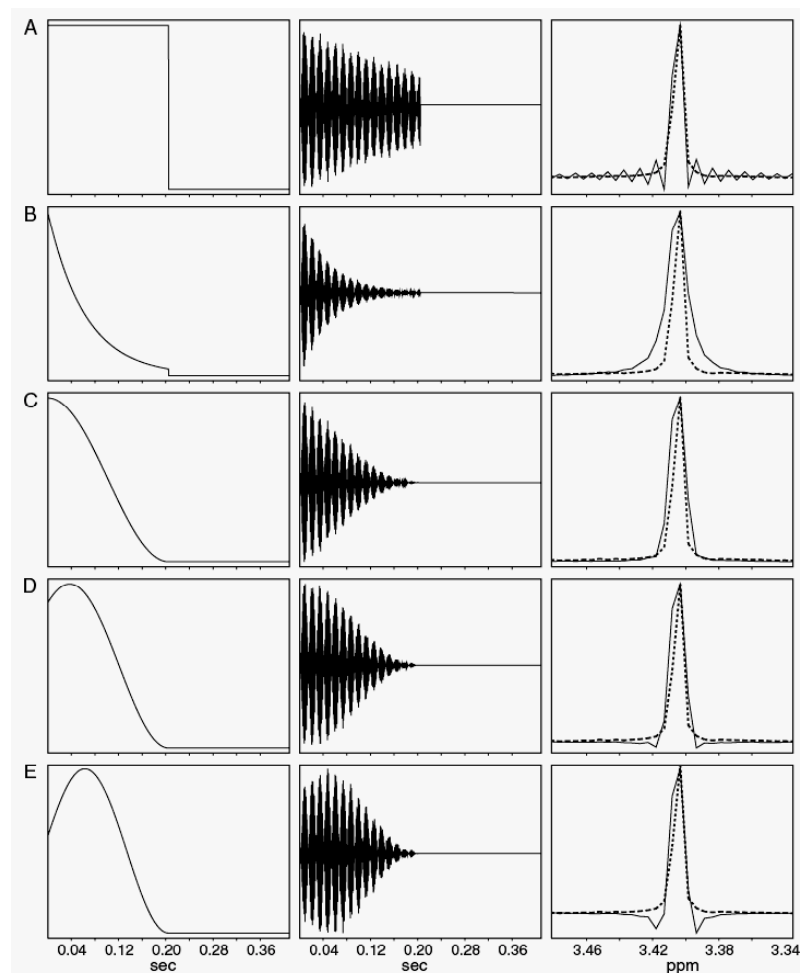
3.3.1.2 Lorentz to Gaussian transform

In addition to suppressing truncation artifacts this function converts a Lorentzian lineshape to a Gaussian lineshape. Gaussian lineshapes approach the baseline faster than Lorentzian lineshapes, providing some enhancement in the apparent resolution of the spectrum, making it easier to fit overlapping peaks. The apodization function is:

$$g_{GL}(t) = e^{+t/a} e^{-\frac{t^2}{2}}$$

Figure 3.7. Effect of apodization functions on spectral lineshapes.

The left column shows the apodization function, the center column shows the FID after multiplication by the apodization function, and the right column shows the transformed spectrum, drawn as a solid line. The dotted line in the right-hand panels show the spectrum that would be obtained if the data were collected until it decayed to zero and no apodization function was applied. The natural linewidth of the resonance line, $\Delta\nu$, is 10 Hz. Row A shows the effect of zero-filling. The spectrum is distorted by the convolution with the sinc function. Row B shows the effect of applying an exponential multiplication (EM) with a time constant of 100 msec, equivalent to a broadening of 10 Hz. Note that the sinc ripples are removed, at the expense of an increased linewidth. Rows C, D, and E illustrate the effect of a shifted sine squared window, with phase shifts of 90° , 70° , and 50° , respectively. The 90° shifted sine² curve is equivalent to a cosine² function. Note the decrease in the linewidth of the spectrum as the phase shift of the sine² function decreases. A 50° shifted sine² function (row E) produces a resonance line with nearly the natural line width. The two negative features on either side of the line arise from the convolution of the Fourier transform of the sine² function with the undistorted line. These lobes can be reduced by using linear prediction to increase the apparent acquisition time.



If a is chosen to be equal to T_2 ,
then the modified FID has the following form:

$$g(t) = e^{-\frac{t^2}{2T_2^2}}$$

The Fourier transform of a Gaussian time domain is a Gaussian line:
A mixture of Gaussian and Lorentzian lineshape.

$$G(\omega) = e^{-\frac{\omega^2}{2T_2^2}}$$

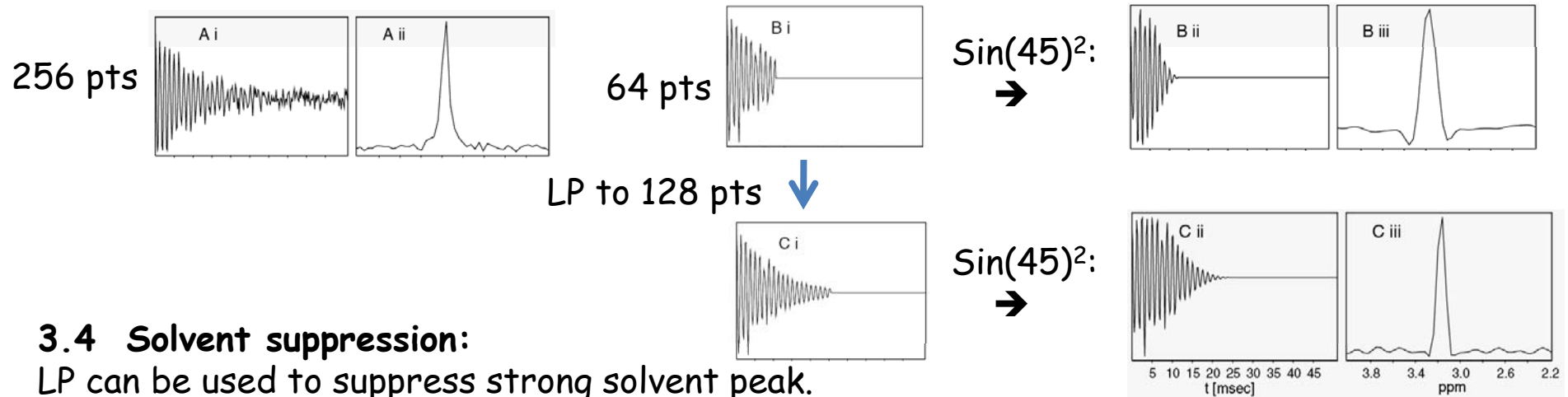
3.3.1.3 Trigonometric Windows:

$$g(t) = \cos^2\left(\frac{\pi}{2T_{ACQ}}t\right)$$

Sine, cosine, $(\sin)^2$, $(\cos)^2$ and their phase shifted variants.

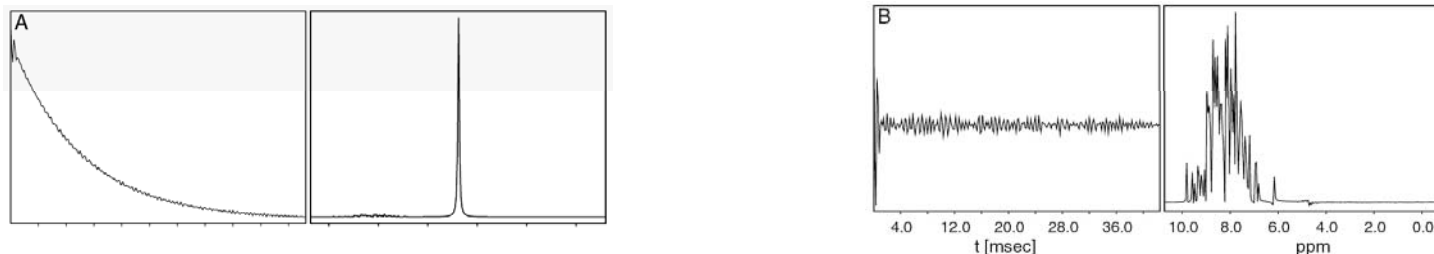
The sine functions are more appropriate for signals that begin at zero, such as in a DQF-COSY experiment, while cosine functions are more useful for signals that have their maximum at $t = 0$ and decay as t increases, i.e. a normal free induction decay.

3.3.2 Using LP & Apodization to increase resolution



3.4 Solvent suppression:

LP can be used to suppress strong solvent peak.



3.4 Spectral artifacts due to intensity errors:

3.5.1 Errors from digital Fourier Transform

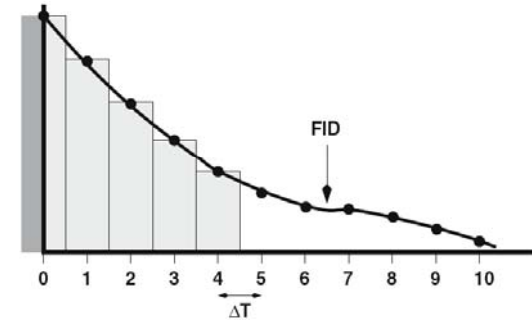
$$S(\omega) = \int F(t) \cos(\omega t) dt$$

$$S(k\Delta\omega) = \sum_{i=0}^{n-1} F_i \cos([k\Delta\omega][i\Delta t]) \Delta t$$

First point is overestimated by a factor of 2

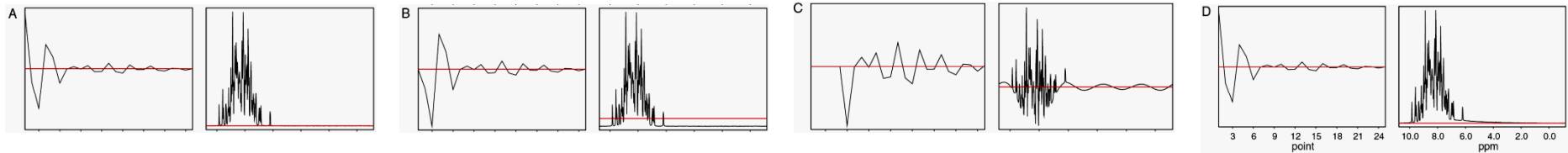
→ Shift half a point or multiply the first pt by 1/2.

Shift the first pt by $\frac{1}{2}$ causes 180 phase shift by make the aliased peak inverted.



3.5.2 Effect of distorted and missing points: (Transmitter dead time)

$$S(k\Delta\omega) = \sum_{i=0}^{n-1} F_i \cos([k\Delta\omega][i\Delta t]) \Delta t = F_0 + F_1 \cos([k\Delta\omega][1 \times \Delta t]) \Delta t + \dots \quad (3.17)$$



A. Undistorted FID;

B, Set 1st pt to zero → DC offset;

C, set 1st 5 pts to zero → rolling baseline;

D, LP of the first few pts

3.5.3 Delayed Acquisition:

A delay in the acquisition of the time domain signal will lead to a frequency dependent, or first-order, phase shift applied to the spectrum.

$$\phi_1 = 360^\circ \times N$$

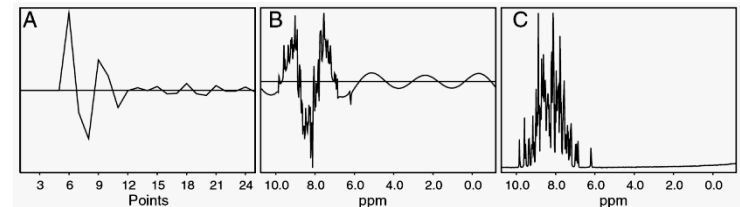


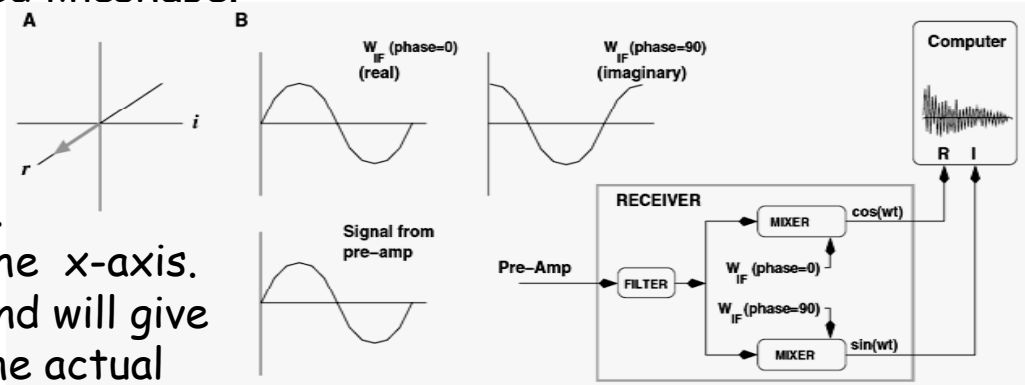
Figure 3.12. Effect of delayed acquisition on the spectrum. The FID (A) has been shifted to the right by 5 points, corresponding to a delay of $\approx 660 \mu\text{sec}$ (sweepwidth = 6000 Hz). The resultant spectrum is shown in B. The correctly phased spectrum is shown in Panel C. A zero order phase shift of -180° and a first-order phase shift of $+1800^\circ$ has been applied to give the phase-corrected spectrum shown in C.

3.6 Phasing of the Spectrum:

The geometrical model defines the phase of the detected signal by the position of the bulk magnetization in the transverse plane at the initiation of signal detection. In this case, the coordinate frame is *defined by the real and imaginary axis of the receiver*. If the signal is aligned along the real axis of the receiver then it has a phase shift of zero and a pure absorption spectrum will be observed. Conversely, if the signal is aligned along the imaginary axis of the receiver, then it has a phase shift of 90° and a dispersion curve will be observed. Signals that lie elsewhere will have a mixed lineshape.

Figure 3.13. Geometric and electronic description of the signal phase.

The real axis of the receiver has been arbitrarily defined to be along the x-axis. The bulk magnetization is aligned along the x-axis. This signal will have a phase shift of 0° and will give a pure absorption mode lineshape. In B, the actual signals that enter the receiver are shown. If the

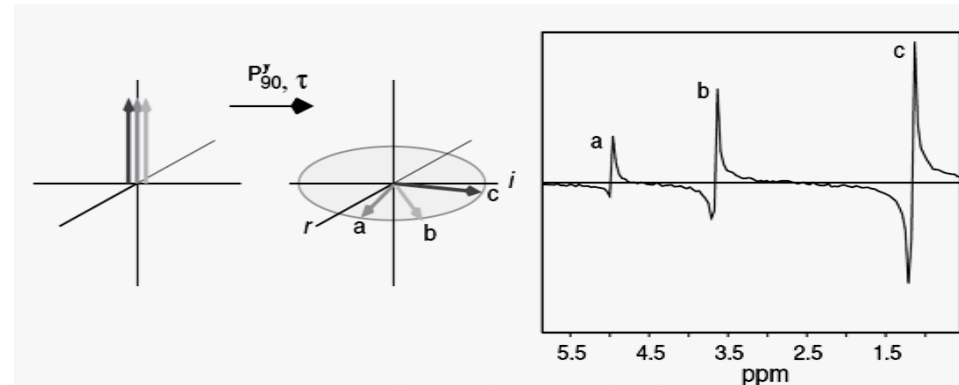
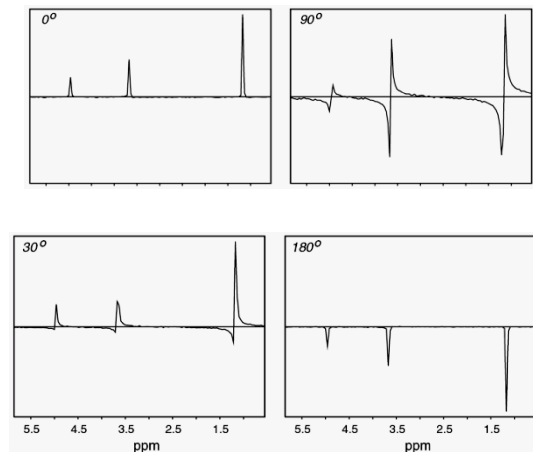


phase of the pre-amp signal is the same as the phase of W_{IF} (phase=0), then the phase shift of the signal is defined to be zero. However, the notion that the receiver phase actually defines the orientation of a coordinate frame, although convenient and of practical use, is incorrect. The phase of the signal is correctly described as the phase difference between the signal that enters the receiver and the intermediate frequency (W_{IF}). When the signal from the pre-amp enters the receiver it is split into two signals. One of these is mixed with W_{IF} that has not been phase shifted, while the other portion is mixed with W_{IF} that has been shifted by 90° . If the detected signal is in-phase with the non-phase shifted W_{IF} then its phase shift is zero. Alternatively, if the detected signal is 90° out of phase with the non-shifted W_{IF} and in-phase with the shifted W_{IF} , then its phase is 90° .

3.6.1 Origin of Phase Shifts

There are several factors that produce a phase shift of the signal:

- 1. Electronic effects:** As the signal progresses from the probe to the digitizer it is amplified and mixed with other signals. These steps introduce a shift in the phase of the signal that will depend on, among other things, the receiver gain and the frequency of the signal. To first-order, these shifts are linear with frequency.
- 2. Off-resonance effects:** Consider the effect of a 90° pulse along the minus x-axis for on- and off-resonance spins. The pulse will rotate the on-resonance spins to the y-axis. If we assume the y-axis of the receiver is the real axis, the phase of on-resonance spins will be zero. Spins that resonate at a lower frequency than the transmitter will precess about a larger effective field, and will end up behind the y axis after the pulse, equivalent to a negative phase shift. Spins that resonate at a higher frequency will end up in front of the y-axis after the pulse, representing a positive phase shift. Again, the phase shift is proportional to the resonance frequency.
- 3. Delay in acquisition of the signal:** It is impossible to collect the signal immediately after the pulse because of transient signals that remain in the probe after a high power RF-pulse. These transients are several times as intense as the real signal, thus it is necessary to wait 10-20 μsec before acquisition of the signal. This delay is often called the receiver dead time. A delay of τ , will lead to a phase shift of ω_{ST} in the detected signal.



First order phase shift

3.6.2 Applying Phase Corrections

Signal with non-zero phase:

$$S(t) = e^{i\omega t} e^{-t/T_2} e^{i\phi(\omega)}$$

FT of $S(t)$: $h_r(\omega) = \cos(\phi)g_r - \sin(\phi)g_i$ $h_i(\omega) = \sin(\phi)g_r + \cos(\phi)g_i$

If we apply a phase correction by adding: $\cos(\phi)h_r(\omega)$ to $\sin(\phi)h_i(\omega)$ to give :

$$\cos^2(\phi)g_r - \cos(\phi)\sin(\phi)g_i + \sin^2(\phi)g_r + \cos(\phi)\sin(\phi)g_i = g_r$$

We obtain a spectrum with pure absorption.

3.7 Chemical Shift Referencing:

$$\delta = \frac{\nu - \nu_o}{\nu_o} \times 10^6$$

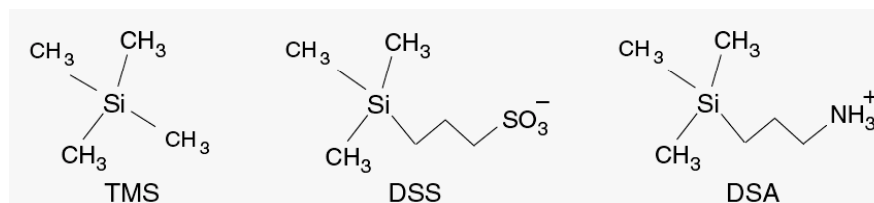


Table 3.2. Compounds for chemical shift referencing. The chemical shift of each compound relative to DSS is indicated, as is the effect of temperature and pH on the resonance line position. This information was obtained from [166].

3.8 Exercises

Compound	Chemical Shift	Effect of pH	Effect of Temperature
¹H Reference Compounds			
TMS	0.000	none	none
DSS/DSA	0.000	none	none
Acetone	2.218	none	none
HDO (25 °C)	4.766	-2 ppb/pH	-11.9 ppb/°C
¹³C Reference Compounds			
TMS	1.70	none	-4 ppb/°C
DSS/DSA	0.00	none	none
NaAcetate	26.10	none	none
Acetone	33.00	none	none
¹⁵N Reference Compound			
NH ₃ (liq., 25 °C)	0.0	n.a.	40 ppb/°C

Chemical Shift Referencing: The ^1H chemical shift was referenced to 2,2-dimethyl-2-Silapentane-5-sulfonate (DSS) at 0 ppm. The ^{15}N and ^{13}C chemical shift values were referenced using the consensus ratio of Ξ of 0.101329118 and 0.251449530 for $^{15}\text{N}/^1\text{H}$ and $^{13}\text{C}/^1\text{H}$, respectively

(Wishart and Case, *Method. Enzymol.* 338, 3-34 (2001))

TABLE I
IUPAC/IUBMB RECOMMENDED Ξ (XI) RATIOS FOR INDIRECT
CHEMICAL SHIFT REFERENCING IN BIOMOLECULAR NMR^a

Nucleus	Compound	Ξ Ratio
^1H	DSS	1.000 000 000
^{13}C	DSS	0.251 449 530
^{15}N	Liquid NH_3	0.101 329 118
^{19}F	CF_3COOH	0.940 867 196
^{31}P	$(\text{CH}_3)_3\text{PO}_4$	0.404 808 636

^a Relative to DSS.

Ξ ratio (Nucleus-specific frequency ratio: Determine the precise ^1H resonance frequency of DSS then multiply this frequency by Ξ of a particular nucleus one obtains the exact resonance frequency reference at 0 ppm of that nucleus.